Supplementary materials

Phase Controlled Synthesis of Pt Doped Co Nanoparticle Composites Using a Metal-Organic Framework for Fischer–Tropsch Catalysis

Atanu Panda†[1], Euisoo Kim†[1], Yong Nam Choi[2], Jihyun Lee[1], Sada Venkateswarlu*[1], Minyoung Yoon*[1]

[1] Department of Nanochemistry, Gachon University, Sungnam 13120, Republic of Korea.
[2] Neutron Science Division, Korea Atomic Energy Research Institute, Daejeon 34057, Republic of Korea
* Correspondence: venkisada67@gmail.com (S.V.); myyoon@gachon.ac.kr (M.Y.)
† Both authors equally contributed to this work.

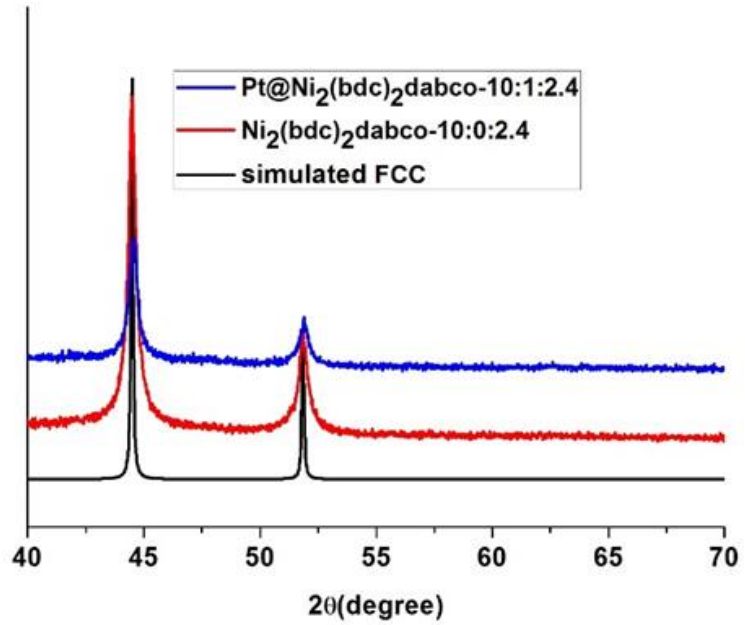

Figure S1. PXRD analysis after carbonization of Pt@Ni/C and Ni/C at 800 ℃ for 4 h under Argon.

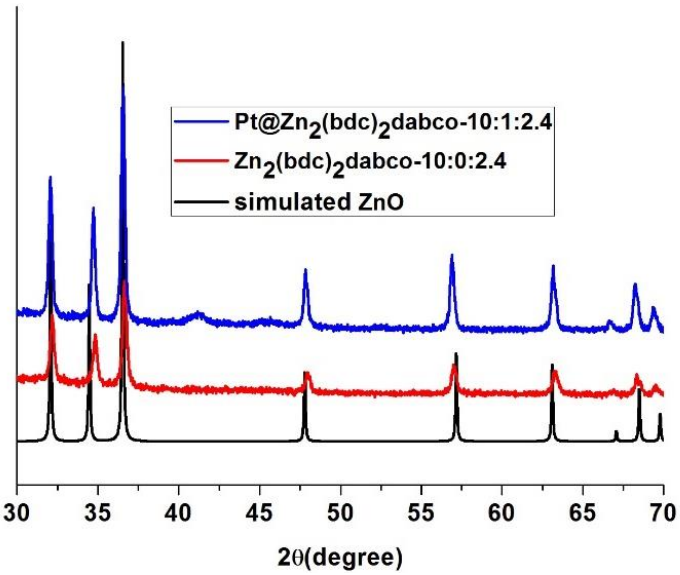

Figure S2. PXRD analysis after carbonization of Pt@Zn/C and Zn/C at 800 ℃ for 4 h under Argon.

Table S1. Elemental analysis of Pt@M/C and M/C (M = Co, Ni, Zn).

Catalysts	C/ %	H/ %	N/ %	S/ %
Pt@Co_2(bdc)$_2$dabco10:1:2.4	32.59	0.25	0.00	0.00
Co_2(bdc)$_2$dabco10:0:2.4	34.41	0.85	0.14	0.00
Pt@Ni_2(bdc)$_2$dabco10:1:2.4	17.06	0.25	0.53	0.00
Ni_2(bdc)$_2$dabco10:0:2.4	17.15	0.12	0.48	0.00
Pt@Zn_2(bdc)$_2$dabco10:1:2.4	30.65	1.05	0.02	0.00
Zn_2(bdc)$_2$dabco10:0:2.4	31.64	0.85	0.02	0.00

Table S2. XPS analysis Pt@M/C and M/C (M = Co, Ni, Zn).

Catalysts	C 1s %	Co 2p %	N 1s %	O 1s %	Pt 4f %
Pt@Co_2(bdc)$_2$dabco10:1:2.4	85.7	1.6	0.7	11.9	0.1
Co_2(bdc)$_2$dabco10:0:2.4	80.4	3.8	0.7	15.1	0.0
Pt@Ni_2(bdc)$_2$dabco10:1:2.4	80.8	2.7	1.8	14.6	0.1
Ni_2(bdc)$_2$dabco10:0:2.4	83.6	3.3	1.6	11.5	0
Pt@Zn_2(bdc)$_2$dabco10:1:2.4	65.7	12.3	0.6	20.9	0.5
Zn_2(bdc)$_2$dabco10:0:2.4	71.7	10.8	0.5	17	0

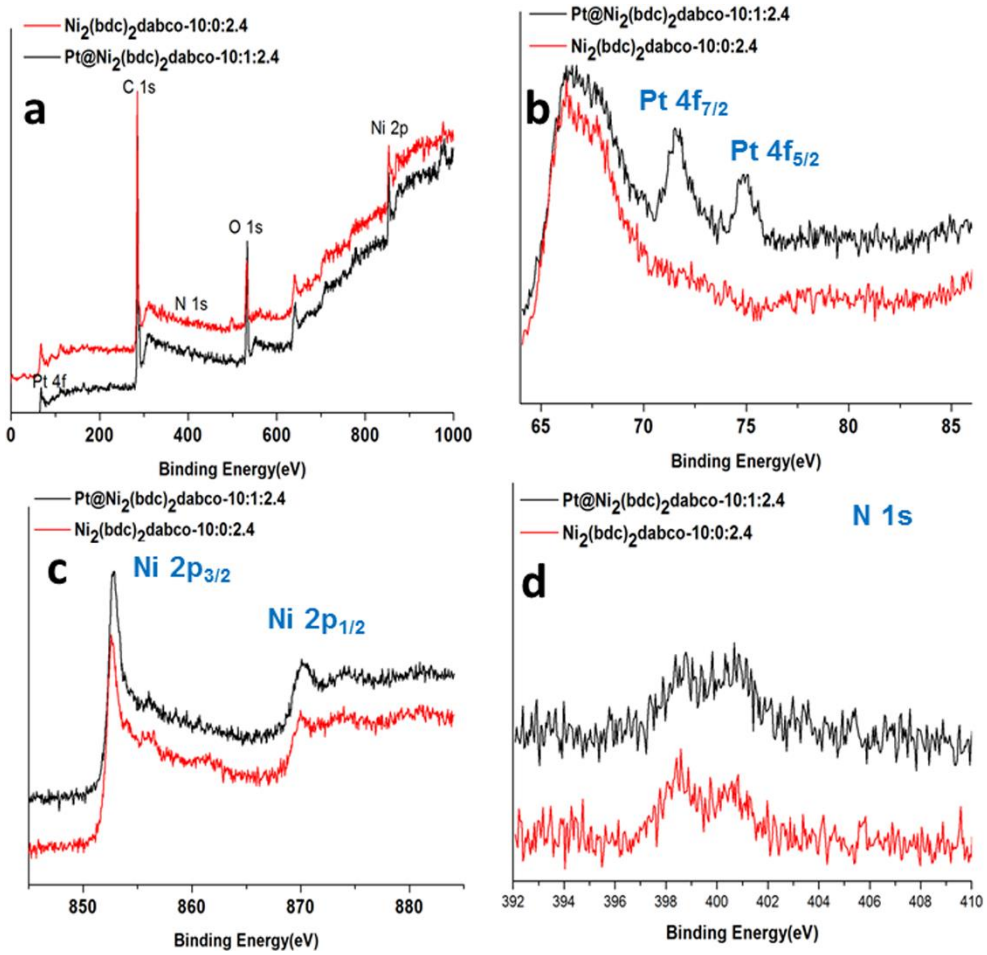

Figure S3. XPS analysis of Ni/C and Pt@Ni/C (a) total survey of XPS, (b) deconvolution XPS of Pt 4f, (c) deconvolution XPS of Ni 2p and (d) deconvolution XPS of N 1s.

Figure S3a shows the survey scan spectrum of the XPS of Ni/C(10:0:2.4) (red line) indicating the peaks at 284, 530 and 852 eV corresponding to the presence of C 1s, O 1s and Ni 2p. Figure S3a displays the survey scan spectrum of the XPS of Pt@Ni/ (10:1:2.4) (black line) showing the additional peak at 75 eV corresponding to the presence of Pt in the composite. The two characteristic peaks of Pt 4f at 71.8 eV and 75.6 eV in Figure S3b indicates the presence of metallic platinum on the surface of the Pt@Ni/C, which suggests the presence of platinum on the surface of the composite. The peaks at 852.7 eV and 870.1 eV corresponds to Ni $2p_{3/2}$ and Ni $2p_{1/2}$ (Figure S3c), and a small peak at 855.9 eV indicating the presence of Ni_2O_3 [S1].

Figure S3d clearly shows the presence of N 1s with a peak at 400.56 eV.

The survey spectrum of the XPS of Zn_2/C(10:0:2.4) (red line) indicates the peaks at 284, 530 and 1022 eV corresponding to the presence of C 1s, O 1s and Zn 2p (Figures S4a). Figure S4a displays the survey spectrum of the XPS of Pt@Zn_2/C(10:1:2.4) (black line) showing an additional peak at 75 eV corresponding to the Pt in the composite. The two characteristic peaks of Pt 4f at 71.6 eV and 75.5 eV in the Pt@Ni/C indicate the presence of metallic platinum on the surface of the catalyst. The peaks at 1022 and 1045.5 eV correspond to Zn $2p_{3/2}$ and Zn $2p_{5/2}$, respectively [S2]. In addition, XPS analysis of Pt@Co/C(10:1:2.4) confirms the presence of Pt (0.1 wt %) on the surface of the catalyst (Table S2).

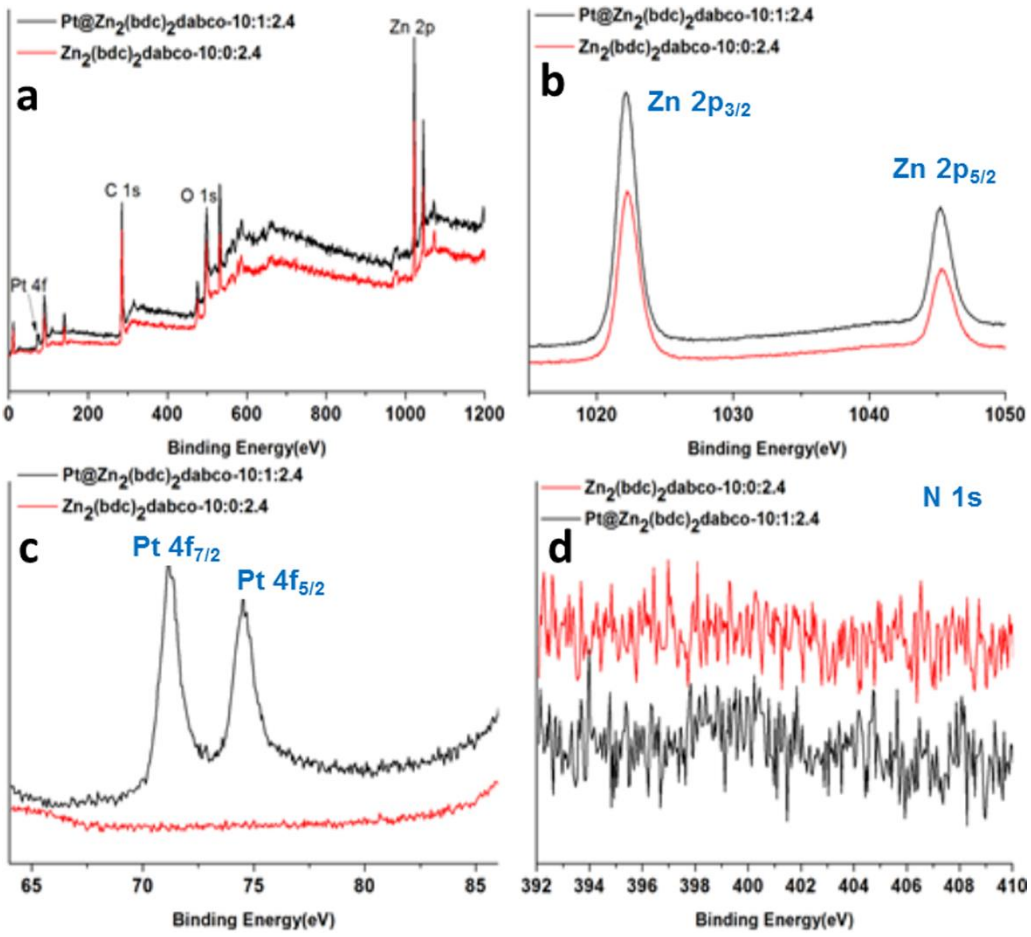

Figure S4. XPS analysis of Zn/C and Pt@Zn/C (a) total survey of XPS, (b) deconvolution XPS of Pt 4f, (c) deconvolution XPS of Zn 2p and (d) deconvolution XPS of N 1s.

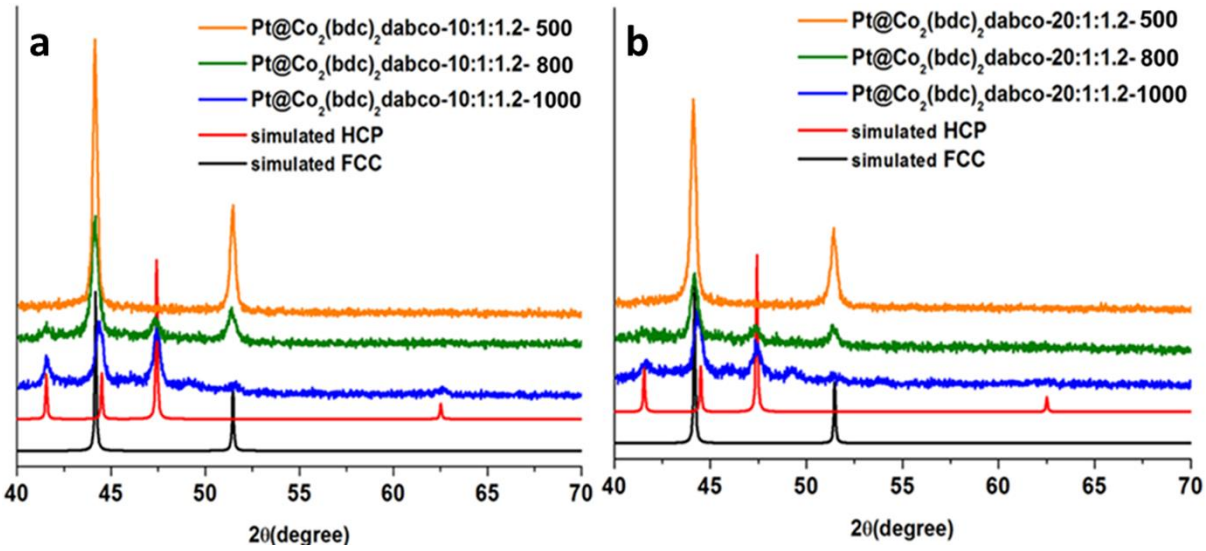

Figure S5. PXRD analysis of (a) Pt@Co/C(10:1:1.2) and (b) Pt@Co/C(20:1:1.2) at different carbonization temperatures.

Table S3. Different carbonization temperature of Pt@Co/C(10:1:2.4).

Carbonization temperature			
	500 ℃	800 ℃	1000 ℃
FCC %	49	82	100
HCP %	51	17.9	0

Table S4. Different carbonization time of Pt@Co/C(10:1:2.4) at fixed temperature of 800 ℃.

$Pt@Co_2(bdc)_2$ (dabco) 10:1:2.4						
Time	**4 h**	**6 h**	**9 h**	**12 h**	**18 h**	**24 h**
FCC %	12 %	39 %	51 %	78.4 %	81.5 %	82 %
HCP %	88 %	61 %	49 %	21.6 %	18.5 %	18 %

Table S5. ICP-AES analysis of Pt@Co@C and Co@C.

$Pt@Co_2(bdc)_2(dabco)$		
	Co	Pt
Before	0.333 ppm	0.02 ppm
After	0.332 ppm	0.02 ppm
$Co_2(bdc)_2(dabco)$		
	Co	Pt
Before	0.165 ppm	0.00 ppm

After	0.154 ppm	0.00 ppm

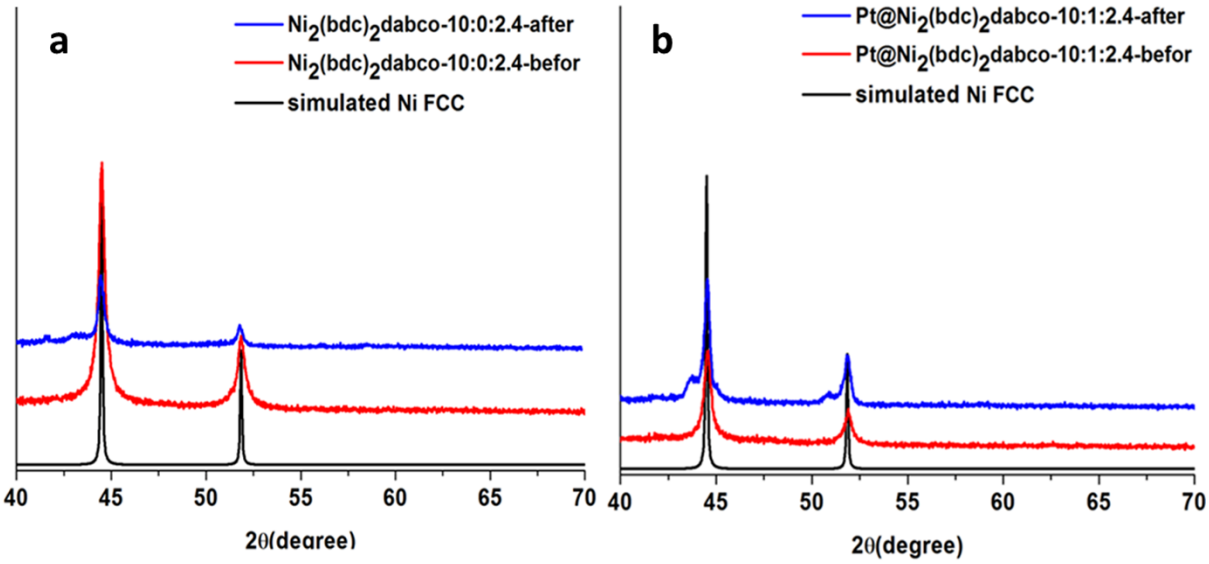

Figure S6. PXRD analysis of (a) Ni/C and (b) Pt@Ni/C before and after FTS.

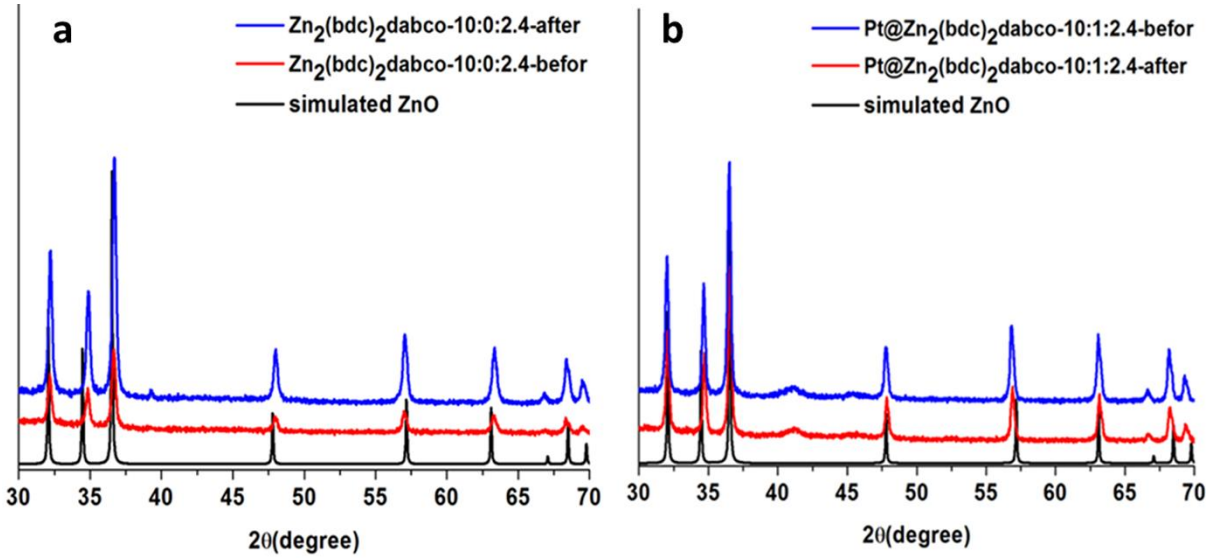

Figure S7. PXRD analysis of (a) Zn/C and (b) Pt@Zn/C before and after FTS.

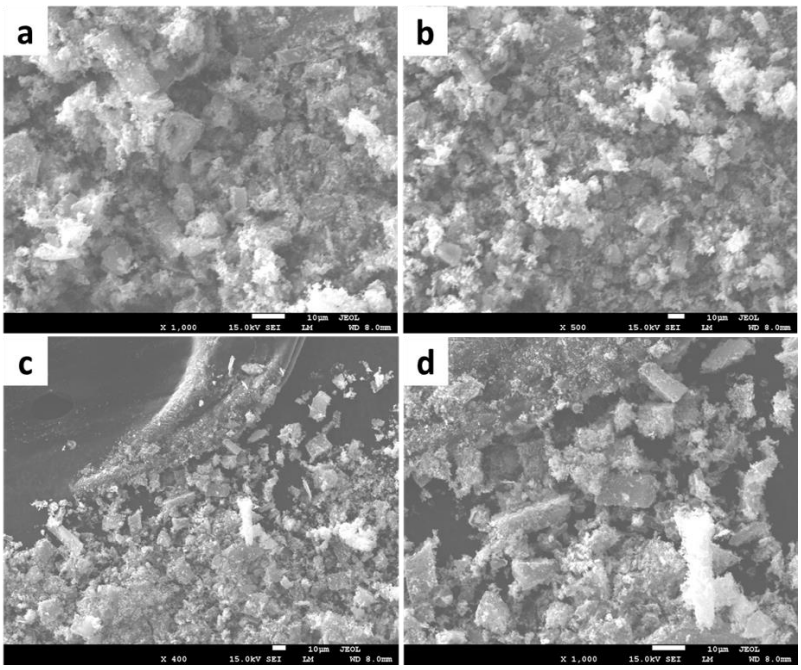

Figure S8. SEM images of (a, b) Co/C before catalytic reaction and (c, d) after catalytic reaction.

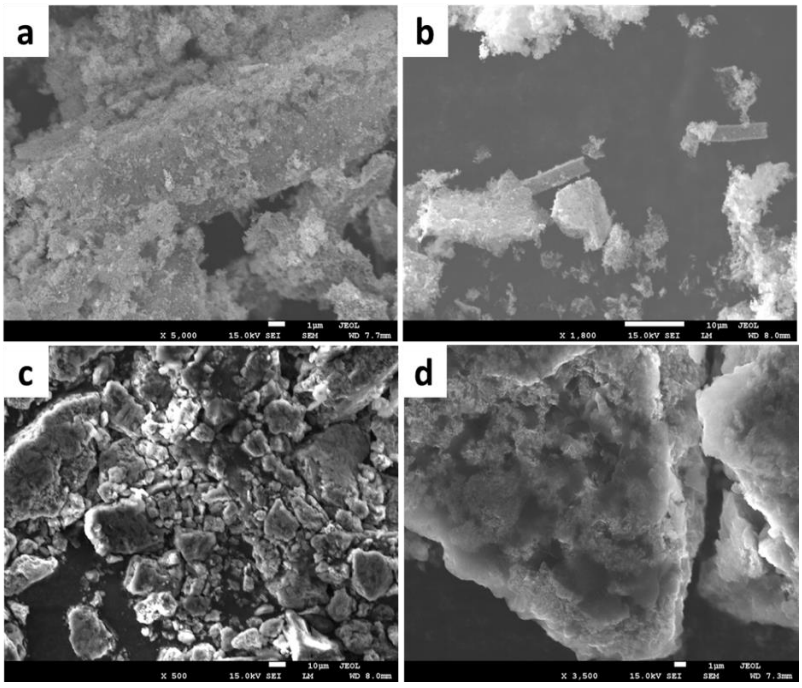

Figure S9. SEM images of (a, b) Pt@Co/C(10:1:2.4) before catalytic reaction and (c, d) after catalytic reaction.

Table S6. Catalytic activity and reaction condition comparison table

Catalyst	Temperature (℃)	Pressure (MPa)	Co weight (%)	Time (h)	CO Conversion (%)	C_2-C_4	C_5	CH_4	References
Fe-BTC derived Fe@C	340	2	-	90	14.6	29	NA	14.6	[3]
Fe-MIL-88B	300	2	-	80	33.8	25.1	63.4	33.8	[4]
Co@MIL-53(Al)	240	2	5.0	20	23.8	13.5	67.7	13.3	[5]
ZIF-67 derived Co@NC	230	3	25	100	10	37	31	22	[6]
Co-MOF-74 derived Co@C	230	3	19.0	100	30	10	65	18	[6]
Co_3O_4-m-SiO_2	220	2	20.0	10	364	6.18	57.6	15.8	[7]
Pt@Co_2(bdc)$_2$(dabco)	250	1	1.6	100	35	21	2.09	76	This work

References

[S1] Chen, Y.S.; Kang, J.F.; Chen, B.; Gao, B.; Liu, L.F.; Liu, X.Y.; Wang, Y.Y.; Wu, L.; Yu, H.Y.; Wang, J.Y.; Chen, Q. Microscopic mechanism for unipolar resistive switching behaviour of nickel oxides. *J. Phys. D.* **2012**, *45*, 065303.

[S2] Patil, S.S.; Mali, M.G.; Tamboli, M.S.; Patil, D.R.; Kulkarni, M.V.; Yoon, H.; Kim, H.; Al, Deyab, S.S.; Yoon, S.S.; Kolekar, S.S.; Kale, B.B. Green approach for hierarchical nanostructured Ag-ZnO and their photocatalytic performance under sunlight. *Catal. Today* **2016**, *260*, 126-134.

[S3] Santos, V.P.; Wezendonk, T.A.; Jaen, J.J.D.; Dugulan, A.I.; Nasalevich, M.A.; Islam, H.U.; Chojecki, A.; Sartipi, S.; Sun, X.; Hakeem, A.A.; Koeken, A.C. Metal organic framework-mediated synthesis of highly active and stable Fischer-Tropsch catalysts. *Nat. Comm.* **2015**, *6*, 6451-6455.

[S4] Wezendonk, T.A.; Santos, V.P.; Nasalevich, M.A.; Warringa, Q.S.; Dugulan, A.I.; Chojecki, A.; Koeken, A.C.; Ruitenbeek, M.; Meima, G.; Islam, H.U.; Sankar, G. Elucidating the nature of Fe species during pyrolysis of the Fe-BTC MOF into highly active and stable Fischer–Tropsch catalysts. *ACS Catal.* **2016**, *6*, 3236-3247.

[S5] Isaeva, V.I.; Eliseev, O.L.; Kazantsev, R.V.; Chernyshev, V.V.; Davydov, P.E.; Saifutdinov, B.R.; Lapidus, A.L.; Kustov, L.M. Fischer–Tropsch synthesis over MOF-supported cobalt catalysts (Co@ MIL-53 (Al)). *Dalton Trans.* **2016**, *45*, 12006-12014.

[S6] Qiu, B.; Yang, C.; Guo, W.; Xu, Y.; Liang, Z.; Ma, D.; Zou, R. Highly dispersed Co-based Fischer–Tropsch synthesis catalysts from metal–organic frameworks. *J. Mater. Chem. A* **2017**, *5*, 8081-8086.

[S7] Xie, R.; Li, D.; Hou, B.; Wang, J.; Jia, L.; Sun, Y. Silylated Co_3O_4-m-SiO_2 catalysts for Fischer–Tropsch synthesis. *Catal. Comm.* **2011**, *12*, 589-592.